MOLECULAR AND CELLULAR BIOLOGY, Aug. 1994, p. 5371–5383
0270-7306/94/$04.00+0

Vol. 14, No. 8

Transcriptional Suppression of the Human T-Cell Leukemia Virus Type I Long Terminal Repeat Occurs by an Unconventional Interaction of a CREB Factor with the R Region

XIAO XU,[1] DAVID A. BROWN,[1] ISAO KITAJIMA,[1]† JAMES BILAKOVICS,[1]‡ LARA W. FEY,[1] AND MICHAEL I. NERENBERG[1,2]*

Department of Neuropharmacology[1] and Department of Molecular and Experimental Medicine,[2] The Scripps Research Institute, La Jolla, California 92037

Received 2 September 1993/Returned for modification 24 November 1993/Accepted 27 April 1994

To analyze regulation of the human T-cell leukemia virus type I (HTLV-I) long terminal repeat (LTR), cell lines were generated from LTR-*tax* × LTR–β-galactosidase (β-Gal) doubly transgenic mouse fibroblastic tumors. The HTLV-I LTR directs expression of both the *tax* and *lacZ* genes, and Tax up-modulates both promoters in primary cells. However, once cells were transformed by *tax*, β-Gal but not *tax* expression was suppressed. Supertransformation of these cells with v-*src* suppressed both β-Gal and *tax* expression. This suppression was reversed by treatment with the tyrosine kinase inhibitor herbimycin A or protein kinase A inhibitor H8. Electrophoretic mobility shift assays demonstrated augmented binding in the R but not U3 region. This binding was competitively inhibited by a high-affinity CREB oligodeoxynucleotide and supershifted with a specific CREB antibody. Treatment of cells with the cyclic AMP analog dibutyryl cyclic AMP also transiently increased the R region binding dramatically. In vitro DNase I footprint analysis identified a protein-binding sequence in the R region which corresponded with suppression. However, this target sequence lacked a conventional CREB-binding site. A 70.5-kDa DNA-binding protein was partially purified by affinity chromatography, along with a 49-kDa protein which reacted with CREB-specific sera. These data demonstrate that HTLV-I LTR suppression is associated with CREB factor binding in the R region, probably by direct interaction with a 70.5-kDa protein, and provide a novel mechanism for maintenance of viral latency.

Human T-cell leukemia virus type I (HTLV-I) has been identified as the etiologic agent of adult T-cell leukemia/lymphoma (reviewed in references 40 and 64). A hallmark of HTLV-I infection is its latency. Adult T-cell leukemia/lymphoma develops after a characteristically long latent period of 20 or more years after initial exposure (40). The proviral genome is readily found in the DNA of primary leukemic lymphocytes (56, 65). However, leukemic cells do not express significant levels of viral antigens unless they are cultured in vitro in the presence of mitogens (16, 36). Both methylation and partial deletion of the viral genome have been associated with in vivo latency (55), but the factors that initiate latency are poorly understood.

Specific interaction of host cell transcription factors with the U3 portion of the HTLV-I long terminal repeat (LTR) is crucial in regulating viral expression (reviewed in reference 22). The 5′ U3 region contains a transcriptional enhancer composed of 21-bp repeat elements (Tax response elements) (18, 46, 49, 54) and sequences homologous to other transcriptional factor-binding motifs such as AP-1 (47, 66), Ets1 (11, 21), Sp-1 (21, 47), and AP-2 (38). The virus-encoded Tax transactivator recently has been shown to increase the in vitro DNA-binding activity of multiple ATF proteins and many other bZIP proteins such as AP-1 and CREB (17, 60, 63), which positively regulate expression of viral mRNA by interacting with DNA-binding motifs in this region (11, 18, 22, 38, 46, 66).

The role of the R region in transcriptional regulation of HTLV-I is still not clear. An early report by others suggested protein-binding activities on the DNA of the R region (34). Recently, our laboratory has mapped the entire R region by in vivo footprinting, revealing multiple specific DNase I-protected regions (6). The R region is thought to function mostly independently of Tax and to increase the level of gene expression when placed downstream of the simian virus 40 promoter (39). An element at the boundary of the R-U5 region was proposed to control virus basal gene expression (30), though this same region represses HTLV-I gene transcription in the presence of the human cytomegalovirus IE2 protein (20).

To study regulation of the HTLV-I LTR in vivo, we have used transgenic models. In previous publications (27, 41, 42, 44), we have described an HTLV-I LTR-*tax* transgenic mouse model which was established by placing the *tax* gene downstream of the U3 and R regions of the viral LTR. Tax protein expression was controlled by the viral LTR and was therefore subject to *tax*-mediated autoregulation. This model reproduced many aspects of transcriptional latency. The mice showed low to absent levels of transcription at birth. With aging, they expressed *tax* in scattered cells of skeletal muscle, fibroblasts, chondrocytes, and salivary glands.

In this study, we have used cell lines generated from LTR-*tax* × LTR–β-galactosidasé (β-Gal) doubly transgenic

* Corresponding author. Mailing address: Department of Neuropharmacology and Department of Molecular and Experimental Medicine, The Scripps Research Institute, CVN-10, 10666 N. Torrey Pines Rd., La Jolla, CA 92037. Fax: (619) 554-6465. Electronic mail address: michaeln@riscsm.scripps.edu.

† Present address: Department of Laboratory Medicine, Kagoshima University School of Medicine, Kagoshima, Japan.

‡ Present address: Ligand Pharmaceuticals, La Jolla, Calif.

mouse fibroblastic tumors to study transformation and induced suppression in greater detail and compared these cell lines with HTLV-I-transformed human lymphocytes.

MATERIALS AND METHODS

Cell lines. (i) *tax*-transformed fibroblasts. A variety of cell lines were established from fibrosarcomas in LTR-*tax* transgenic mice. One such line which has served as a prototype for *tax* transformation studies was cloned from single cells via Terisaki plates and designated line B (31, 32). Similar *tax*-transformed primary fibroblasts were derived from LTR-*tax* × LTR–β-Gal tumors (7). A prototypic culture was termed LTL. 5-Bromo-4-chloro-3-indolyl-β-D-galactopyranoside (X-Gal) staining (35) revealed two cell populations within this culture, a strongly β-Gal-positive population (approximately 90% of the cells in primary culture) and a β-Gal-negative population. These are referred to as LTL-blue and LTL-white cells, respectively. Pure populations of these cells were prepared by fluorescence-activated cell sorting (FACS) using a fluorescent β-Gal substrate (35). Briefly, single-cell suspensions (10^8 cells) were prepared, preheated to 37°C, and then pulsed with 2 mM fluoresceine di-β-galactoside for 1 min. Cells were chilled, diluted, and exposed to 1 μg of propidium iodide per ml. The reaction was terminated with 1 mM phenylethyl-β-D-thiogalactoside. Energy gates which allowed clean separation of the two populations were determined.

(ii) LTL cells transformed by v-*src*. High-passage LTL-white cells were transformed by the v-*src*-expressing plasmid pSrc11 (57), obtained from the laboratory of Inder Verma (Salk Institute, La Jolla, Calif.), or by direct transformation with the SR strain of Rous sarcoma virus (RSV; obtained from the American Type Culture Collection, Rockville, Md.) by a method described previously (14). RSV SR-transformed 3T3 cells were also obtained from the Verma laboratory. Transformations were done by Lipofectin (GIBCO/BRL, Bethesda, Md.) transfection. After 10 days, formed foci were selected and passaged four times. These cells were named LTL/src, and five independent lines were characterized. For RSV SR transformation, 10^4 PFU of virus per ml was added to cells pretreated with Polybrene (20 μg/ml). Virus was removed after a 2-h incubation, and cells were treated with 50% polyethylene glycol (molecular weight, 1,800) for 1 min. Cells were washed three times prior to culturing. Foci formed after 14 days were selected and passaged four times. These lines were designated LTL/RSV. All cell lines were maintained in Dulbecco modified Eagle medium with 10% fetal calf serum and antibiotics. MT2 producer and MT4 nonproducer cell lines were from the American Type Culture Collection. These lymphocytes were maintained in RPMI 1640 medium containing 10% fetal calf serum and antibiotics.

Use of kinase, phosphatase, and protein synthesis inhibitors in fibroblast cell lines. Herbimycin A (GIBCO/BRL) was prepared as a 1-mg/ml stock solution in dimethyl sulfoxide and stored at −20°C. LTL/src cells were treated for 72 h with herbimycin A at concentrations ranging from 50 to 400 ng/ml. The protein kinase inhibitors H7 and H8 (Seikagaku America, Inc., St. Petersburg, Fla.) were prepared as 10 mM stock solutions in water. LTL/src cells were treated with either H7 or H8 at 10 or 20 μM, respectively, for 72 h. Treatment of cells with okadaic acid, forskolin, or phorbol 12-myristate 13-acetate plus inomycin or cycloheximide (Sigma, St. Louis, Mo.) was for 12 h. The concentration of dibutyryl cyclic AMP (dBcAMP; Sigma) was 1 mM.

MUG assay. The method used has been described elsewhere (35). Briefly, 20,000 cells per well were cultured in 96-well plates overnight prior to treatment with drugs. Cells in each well were preincubated in 105 μl of Z buffer (60 mM $Na_2PO_4 \cdot 7H_2O$, 40 mM $NaH_2PO_4 \cdot H_2O$, 10 mM KCl, 1 mM $MgSO_4 \cdot 7H_2O$ [pH 7.0]) containing 0.1% Triton X-100 for 15 min at room temperature, and then 30 μl of methylumbelliferyl-β-D-galactoside (MUG) stock solution (3 mM MUG [Sigma] in Z buffer) was added at 37°C for 1 h. The reaction was stopped by addition of 300 mM glycine–15 mM EDTA (pH 11.2), and fluorescence was measured on a Titertek Fluoroscan II fluorometer with excitation and emission set to 355 and 460 nm, respectively. Viability of the cells was measured in parallel by the tetrazolium salt [3-(4,5-dimethylthiazol-2-yl)-2,5-diphenylformazan bromide (MTT)] assay (24).

Northern (RNA) blot and Western blot (immunoblot) analyses. Poly(A)$^+$ mRNA was extracted from cells by the FastTrack method (9). Two micrograms of mRNA per lane was electrophoresed on formaldehyde–1.4% agarose gels, transferred to nylon membranes, and subjected to UV fixation. [^{32}P]dATP-labeled cDNA probes for Tax, LacZ, and actin were prepared via PCR amplification of approximately 250-base fragments (32). The cDNA probe for v-*src* mRNA was labeled via the random primer method using [^{32}P]dATP (32). Expression of Tax protein was determined by Western blot analysis as previously described (32).

Nuclear protein analysis. The procedure for preparation of nuclear protein extracts was adapted from a procedure described previously (8). All manipulations were done at 4°C. Nuclei were isolated by homogenization of cells in 0.3 M sucrose–10 mM Tris-HCl (pH 7.9)–10 mM KCl–1.5 mM $MgCl_2$–0.1 mM EDTA–0.5 mM dithiothreitol (DTT)–0.5 mM phenylmethylsulfonyl fluoride (PMSF) and then centrifuged (2,000 rpm). Pelted nuclei were gently suspended in 10 mM Tris-HCl (pH 7.9)–400 mM NaCl–1.5 mM $MgCl_2$–0.1 mM EDTA–5% glycerol–0.5 mM DTT–0.5 mM PMSF. The suspension was stirred for 30 min at 4°C and centrifuged for 45 min at 14,000 rpm. The suspension was collected and dialyzed overnight against dialysis buffer (20 mM Tris-HCl [pH 7.9], 0.1 mM EDTA, 75 mM NaCl, 0.5 mM DTT, 0.5 mM PMSF, 20% glycerol), clarified by centrifugation, quantitated by the Bradford method, and stored at −80°C.

Electrophoretic mobility shift assay (EMSA). Protein-DNA binding reactions were optimized for individual probes and typically made use of 4 μg of total nuclear protein, 0.5 ng of probe, and 1 μg of the nonspecific competitor poly(dI-dC). Mixtures were incubated for 30 min at room temperature in 25 μl of 10 mM Tris (pH 7.5)–75 mM NaCl–10 mM EDTA–7% glycerol–1 mM DTT. The free and protein-bound DNA probe was then resolved by polyacrylamide gel electrophoresis (PAGE) using a 25 mM Tris base–25 mM boric acid–1 mM EDTA buffer at 120 V for 4 h at 4°C in 5% gels. Gels were dried at 80°C and autoradiographed. For competition assays, oligodeoxynucleotides (ODNs) or DNA fragments were added at different concentrations at the same time as probes. For supershift assays, specific antibodies (anti-CREB, obtained from M. Montminy or J. Hoeffler, and anti-c-Jun, from Santa Cruz Biotechnology) or normal rabbit serum was mixed with nuclear proteins for 15 min at room temperature, and then probes and reaction buffer (see above) were added. Probes used were an integral U3 probe (*Sma*I-*Nde*I fragment from −322 to −56), an R region probe (*Nde*I-*Hin*dIII fragment from −56 to +269) (Fig. 3A), CREB ODN, AP-1 target ODN (Fig. 5A) (45, 52), and replicative-form (RF) ODN (Fig. 4D). Probes were end labeled by Klenow polymerase fill-in with [^{32}P]dATP. The specific radioactivity of probes was about 10^8 cpm/μg of DNA.

In vitro DNase I footprint assay. The assay was done as previously described (2). The HTLV-I LTR *Nde*I-*Hin*dIII fragment which contains the entire R region was used as a probe. It was end labeled with Klenow polymerase in the presence of [^{32}P]dATP. The labeled fragment was purified by PAGE and electroeluted. For DNase I footprinting assays, 0.5 to 1.0 ng (about 40,000 cpm) of the probe was incubated for 30 min at room temperature with 100 or 200 μg of nuclear extract in 100 μl of reaction solution (10 mM Tris [pH 7.5], 75 mM NaCl, 1.0 mM EDTA, 1 mM DTT, 7% glycerol); 200 ng of poly(dI-dC) was used as a nonspecific competitor. Then 4 μl of DNase I start buffer (125 mM $MgCl_2$, 62.5 mM $CaCl_2$) was added, followed by mixing with 0.2 μg of DNase I (Promega) for 2 min at room temperature. The reaction was stopped with 4 μl of stop buffer (350 mM EDTA, 195 mM EGTA), extracted with phenol-chloroform, and precipitated with ethanol. Dried DNA pellets were dissolved in 80% formamide, heated for 3 min at 90°C, and analyzed by electrophoresis in 6% polyacrylamide–8.3 M urea sequencing gels. Autoradiography was at −80°C. For specific competition, an ODN which bracketed the footprinted sequence was synthesized (Fig. 4D). This competitor was added into the reaction mixture in increasing amounts from 200 to 800 ng. The reaction conditions and DNase I digestion conditions were as described above.

DNA affinity chromatography. The purification scheme used was as previously described (29). Briefly, preligated R region ODNs (5 to 20 copies of a 25-mer double-stranded ODN [RF]) were coupled to cyanogen bromide-activated Sepharose 4B (80 μg of ODN per ml of resin). DNA-binding protein was partially purified by phosphocellulose fractionation (P11; Whatman) before DNA affinity chromatography. Nuclear extracts prepared from LTL/src cells (described above) were applied to a 5-ml phosphocellulose column equilibrated with buffer D (10 mM *N*-2-hydroxyethylpiperazine-*N'*-2-ethanesulfonic acid [HEPES; pH 7.9], 100 mM KCl, 1.5 mM $MgCl_2$, 0.5 mM DTT, 0.5 mM PMSF, 10% [vol/vol] glycerol). The proteins were eluted from the column with a step gradient of 0.1 to 1.0 M KCl in the same buffer. The binding activity for each fraction was monitored by EMSA, and fractions containing peak DNA-binding activity were pooled and dialyzed. The phosphocellulose-fractionated LTL/src nuclear proteins were premixed with poly(dI-dC) and applied to an RF ODN affinity column preequilibrated with 100 mM KCl in buffer D. Passage through the affinity column was by gravity flow. The resin was washed three times with 100 mM KCl in buffer D, and proteins were eluted with a step gradient of 0.2 to 1.0 M KCl in buffer D. Peak DNA-binding activity fractions were pooled and passed through the affinity column again. Purification and the binding activity were monitored by silver staining, EMSA, and Southwestern (DNA-protein) blot analyses.

Southwestern blot analysis. The method used was described previously (3). After sodium dodecyl sulfate-PAGE (10% gel) of the protein fractions, the gel was incubated in renaturation buffer containing 50 mM KCl, 10 mM Tris-Cl (pH 7.5), 20 mM EDTA, 0.1 mM DTT, and 4 M urea at 4°C for two 1-h washes. Protein transfer to Immobilon membranes was performed electrophoretically in a semidry apparatus at 4°C in buffer containing 25 mM Tris and 192 mM glycine for 1.5 h at 15 V. Nonspecific binding of nucleic acid probes to membranes was blocked by preincubation in 5% dry milk–50 mM KCl–10 mM HEPES (pH 7.9)–0.1 mM EDTA–1 mM DTT at room temperature for 2 h. Then 6×10^6 cpm of RF ODN per ml and 10 μg of poly(dI-dC) per ml were added, and incubation was allowed to proceed at room temperature for 4 h. Specific competition was achieved with 100 ng of each unlabeled competitor ODN per ml, added to the reactions at the same time. Washes were performed at room temperature with the same buffer lacking probe.

RESULTS

Suppression of the HTLV-I LTR promoter in fibroblasts occurs through the protein kinase A (PKA) pathway. In the intact virus, establishment of transcriptional latency is associated with down-modulation of *tax*, since the same promoter directs expression of all viral products. In our LTR-*tax* × LTR–β-Gal doubly transgenic model, we have found that suppression of the LTR–β-Gal promoter may occur despite high levels of constitutive tax expression. To investigate this suppression in greater detail, we established fibroblast cell lines from doubly transgenic tail tumors. A prototypic primary doubly transgenic cell culture was named LTL. FACS analysis of these cells performed with a fluorescent β-Gal analog (Fig. 1A, panel b) confirmed the two populations of fibroblasts seen by X-Gal staining in tissues (7). These populations were purified by fluorescent sorting (Fig. 1A, panels c and d) and were termed LTL-white and LTL-blue, for cells which expressed low and high levels of β-Gal, respectively. Northern blot analysis of the two sublines revealed equivalent levels of *tax* expression, with profound differences in β-Gal mRNA (Fig. 1B). Nuclear run-on experiments (5) revealed that these differences were consistent with differences in initiation of transcription. Cycloheximide induction had minimal effects on expression in either cell type (Fig. 1B). LTL-blue cells showed a slower growth rate, greater contact inhibition, and a tendency to spontaneously convert to LTL-white cells. This finding suggested that suppression of the β-Gal transgene in LTL-white cells may occur as a result of malignant progression.

To assess pathways involved in suppression, we treated LTL-blue cells with a panel of 25 growth factor and signal transduction modulators. Effects of these agents on LTR expression were monitored by a fluorescent MUG β-Gal assay. Of those, only forskolin (a PKA agonist [1, 26]) and okadaic acid (a serine/threonine phosphatase inhibitor [61]) treatment resulted in reproducible suppression of two- and threefold, respectively (Fig. 1C). Combination of these treatments was synergistic (data not shown). None of the PKC agonists or antagonists were shown to affect β-Gal expression (data not shown). These results strongly implicate the PKA pathway in suppression of the β-Gal LTR.

The LTR-*tax* promoter is suppressed by v-Src kinase. Long-term studies with protein kinase drug agonists or inhibitors are complicated by rapid cellular compensation, which diminishes the effects of these drugs (1, 26, 25, 61). In addition, these agents have long-term toxic effects on cells. In an attempt to overcome these limitations, we achieved long-term overexpression of kinase by transfection. Previous studies by others (48) have demonstrated that long-term constitutive overexpression of PKA is associated with arrest of cell growth in many cell lines. PKC augments fibroblast growth but does not cause suppression of the LTR. As an alternative, we introduced the upstream kinase, v-Src, into the cells. Oncogenic v-Src kinase can activate PKC-dependent and -independent pathways (12, 13). Src kinase can also greatly enhance PKA-dependent signalling pathways in murine fibroblasts (37, 51, 59). In addition, it augments rather than attenuates growth of the murine fibroblasts. Infection of RSV SR or cotransfection of a *src*-expressing plasmid followed by neomycin selection yielded high levels of Src protein in the LTL parent cell line.

Results of Northern blot analysis of *src* and *tax* expression in three independent cell lines are shown in Fig. 2A. Corresponding Western blot *tax* analysis is shown in Fig. 2B. Each of the

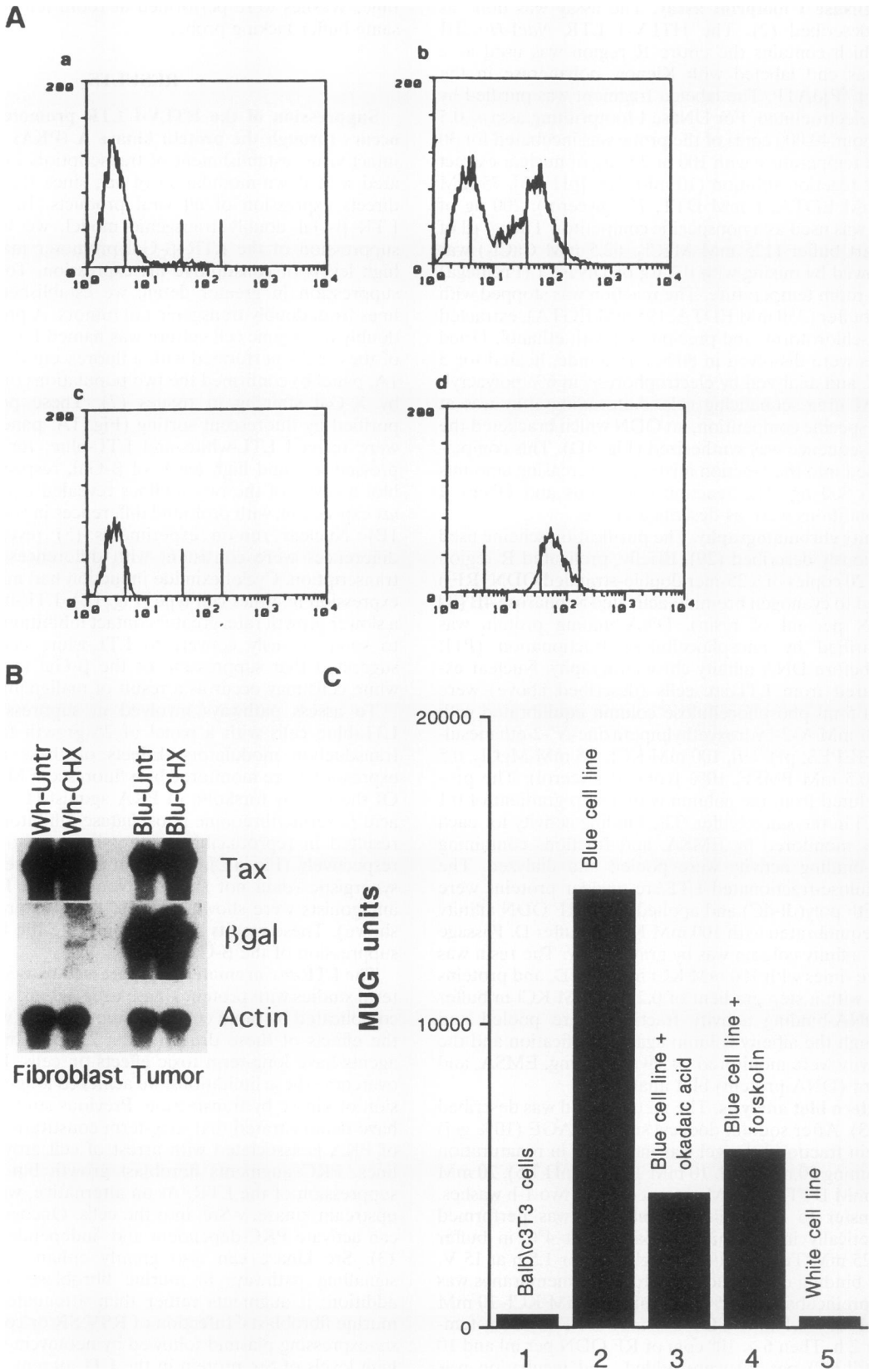

FIG. 1. Characterization of the LTL-blue cell line. (A) Two cell populations were identified and separated by FACS from primary cultures (without [control; a] and with [b] fluorescein di-β-galactoside). The right and left peaks represent the β-Gal-positive and -negative populations respectively. Gates for sorting are indicated. Two populations were then purified and called LTL-blue cells (β-Gal positive) (d) and LTL-white cells

derived cell lines expressed high levels of v-*src* but failed to express *tax* mRNA or protein, indicating successful suppression of even the high-copy LTR-*tax* transgene (40 copies). β-Gal expression (five copies) was also completely suppressed (data not shown). Treatment of these cells with the potent tyrosine kinase inhibitor herbimycin A partially restored *tax* expression, with kinetics similar to those previously demonstrated for *src* inhibition (19) (Fig. 2C). To assess the involvement of PKA as a possible downstream target of *src*, the PKA inhibitor H8 was used (26). Optimal concentrations of this inhibitor produced results similar to those with herbimycin A. No additional derepression was seen with the PKA-PKC inhibitor H7 (26) (Fig. 2D). Incomplete derepression by herbimycin and H8 may be due to additional long-term effects of v-Src kinase which may be partially irreversible. Alternatively, they may result from incomplete inhibition of kinases by these drugs.

Specific protein binding to the HTLV-I LTR R region is associated with suppression. The results described above suggest a direct transcriptional effect of a PKA-sensitive factor on the LTR. As this pathway appears to be different from that mediated by *tax*, it could occur through multiple target sites within the LTR. Thus, comparison of the stable *src*-transformed LTL cells (termed LTL/src) with the parent LTL cell line should allow identification of the relevant transcription factors and LTR target sites. This was accomplished by comparative EMSA using nuclear extracts from the different mouse fibroblast cell lines. As controls, nuclear extracts from BALB/c 3T3 and a well-characterized singly transgenic LTR-*tax* fibrosarcoma, line B (31, 32), were also tested in parallel. DNA probes consisted of radiolabeled fragments encompassing the U3 region (−322 to −56) and the entire R region (−57 to +269) (Fig. 3A).

EMSA results for binding to the U3 region are shown in lanes 1 to 4 of Fig. 3B. Three protein complexes (labeled B1, B2, and B3) were detected. No difference was found between the cell lines in which the LTR-*tax* was activated (Fig. 3B, lane 2 and 3) or suppressed by v-Src kinase (Fig. 3B, lane 4). A minor band between B2 and B3 was found to occur variably in LTL, LTL/src, and BALB/c 3T3 cells and was not specifically competed for. This U3 binding pattern was similar to the shift pattern found in the two control cell lines (Fig. 3B, lanes 1 and 2). Previous reports have identified CREB-, AP-1-, or Ets-like binding sites within U3 (22). We were unable to achieve competition of U3 binding in any of these extracts with high-affinity CREB or AP-1 consensus ODNs even at 500-fold molar excess. Similarly, the R region probe failed to compete for U3 binding. However, the B3 complex was efficiently inhibited by a short Ets1-responsive region-containing sequence (data not shown). In contrast, an unlabeled U3 probe efficiently blocked all three complexes. These results suggest that the U3 region is not a target of PKA-mediated suppression and that CREB and AP-1 complexes are not the major U3-binding proteins in these murine cell extracts.

Results of EMSA using the entire R region as a probe are shown in lanes 5 to 8 of Fig. 3C. Three different protein complexes were detected and designated R1, R2, and R3.

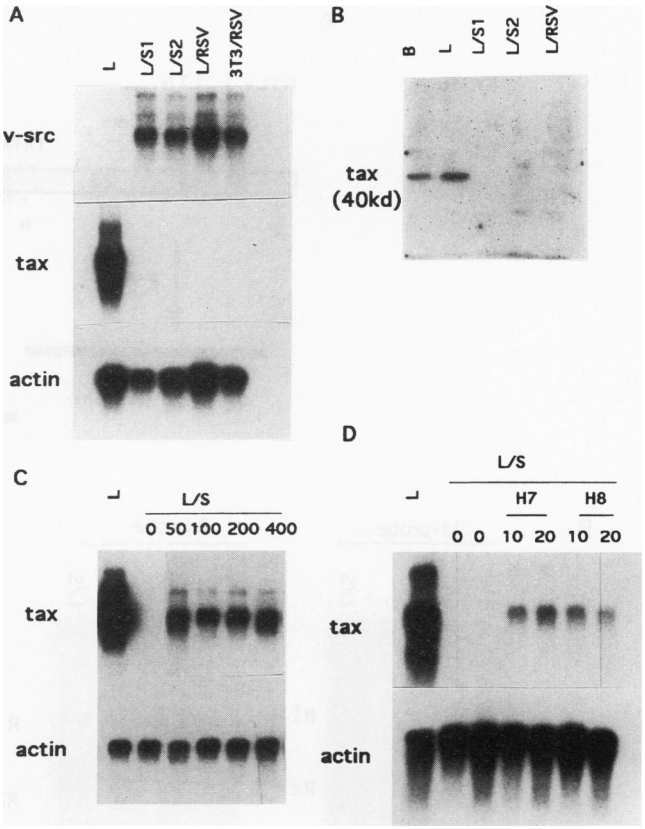

FIG. 2. Suppression of the *tax* LTR by *src* transformation. LTL-white cells were transformed by a v-*src*-expressing plasmid or by RSV. Northern (A) and Western (B) blot analyses were performed on the v-*src*-transformed LTL cell lines. L, LTL parent cell line; L/S1 and L/S2, two separate v-*src*-transformed LTL cell lines; L/RSV, RSV-transformed LTL cell line; 3T3/RSV, RSV-transformed BALB/c 3T3 cell line. *tax* mRNA (A) and Tax protein (B) in v-*src*-transformed cell lines are undetectable. (C) Reversal of suppression with herbimycin. Northern blot analysis of v-*src*-transformed LTL cells was performed after treatment with herbimycin at doses ranging from 0 to 400 μg/ml for 72 h. (D) Reversal of suppression with PKA inhibitors. Northern blot results for H7- and H8-treated v-*src*-transformed cells are shown. H7 and H8 were used at concentrations of 10 and 20 μg/ml. Actin served as a positive control for equal loading.

Complex R3 was seen to be much stronger in the LTL/src nuclear extract than in the parent LTL extract or *tax*-transformed B-line extract. The complex was absent in BALB/c 3T3 cell nuclear extracts. All three complexes were competed for by the unlabeled R fragment but not by the U3 or control pUC fragment (Fig. 3C). This finding suggests that R region binding directly correlates with suppression of transcription and that regulation of the U3 and R regions occurs through binding of different transcription factors.

Since it is possible that these results represent a peculiarity

(β-Gal negative) (c). Panels c and d represent repeat analyses of purified populations. (B) Northern analysis of β-Gal mRNA expression in LTL-blue and LTL-white cell lines confirmed transcriptional suppression of β-Gal but not *tax*. Cycloheximide (CHX) treatment was at 20 μg/ml for 6 h. Actin served as a control for equal loading. (C) Fluorescent (MUG) analysis of β-Gal expression demonstrates suppressive effects of okadaic acid and forskolin. The level of β-Gal expression is represented by fluorescent units; BALB/c 3T3 (column 1) and LTL-white (column 5) cells served as negative controls. Column 3, LTL-blue cells treated with okadaic acid (100 μM); column 4, LTL-blue cells treated with forskolin (100 μM).

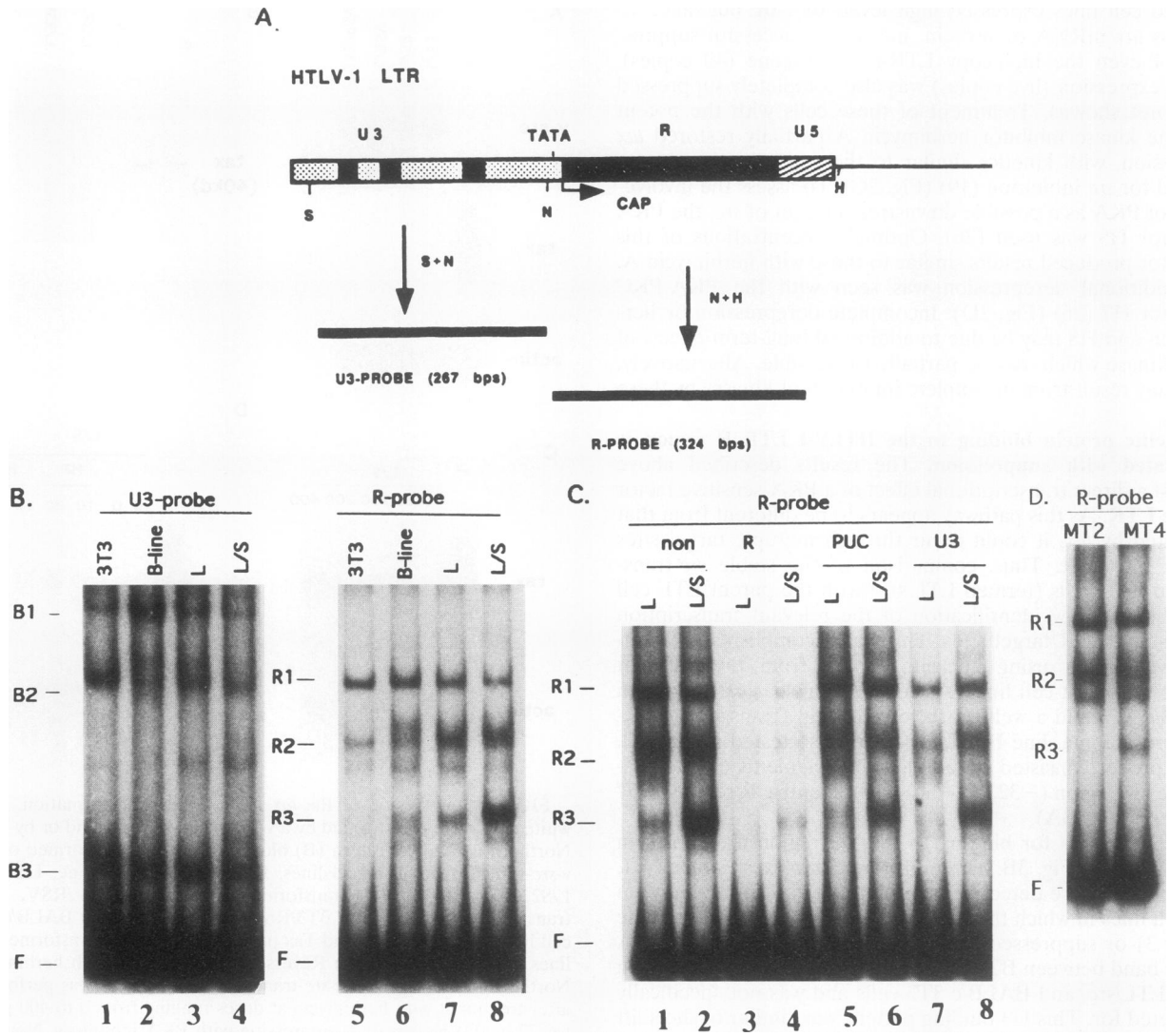

FIG. 3. EMSA analysis of nuclear protein binding to the HTLV-I LTR in v-*src*-transformed, transcriptionally suppressed cells. (A) Derivation of the two EMSA probes. The U3 and R probes were purified from HTLV-1 LTR-*tax* plasmid DNA (40) after digestion with *Sma*I (S) plus *Nde*I (N) or *Nde*I plus *Hin*dIII (H). The size of each probe is indicated. (B) EMSA using radiolabeled U3 and R probes. Protein-DNA complexes are indicated as B1, B2, and B3 for the U3 probe and as R1, R2, and R3 for the R probe. F, free probe. (C) A competition assay was performed with an unlabeled R region (lanes 3 and 4), pUC plasmid DNA (lanes 5 and 6), or U3 region (lanes 7 and 8) fragment. Results of EMSA without competitor are shown. Competition was performed at a 50-fold molar excess. L, parent LTL line; L/S, *src*-transformed LTL cell line. (D) EMSA of MT2 and MT4 nuclear extracts with the R region probe. The corresponding protein-DNA complexes and free (F) are indicated.

of *tax*-transformed mouse cells, similar EMSA analyses were performed in HTLV-I-transformed human lymphocytes. Results of experiments using nuclear extracts obtained from the productively infected cell line MT2 (56) were compared with those from the HTLV-I-infected latent cell line MT4 (55) in Fig. 3D. Latently infected MT4 cells revealed a protein complex identical in mobility to R3 found in LTL/src cells. This complex was not detected in productively infected MT2 nuclear extracts. Again, no reproducible differences between the two cell lines were seen in binding patterns of the U3 region. These results for human lymphocytes confirm those for mouse fibroblasts; i.e., LTR suppression does not involve the U3 region but instead is induced by binding of specific and unique factors within the R region.

The suppressor target is an 18-bp sequence near the R-U5 junction which does not contain a conventional CREB-binding site. To map the site of interaction within the R region, in vitro DNase I footprinting analyses were performed with an end-labeled R region fragment. Results for nuclear extracts from LTL/src cells are compared with those from the parent LTL cell line in Fig. 4A. Lanes 3 to 6 reveal a unique 18-base region strongly protected from DNase I digestion by the LTL/src nuclear extract over a range of concentrations. Protection cannot be detected well in the LTL cell extract at these protein concentrations (Fig. 4A, lanes 7 and 8). This observation corresponds well with the intensity of R3 complex binding seen in EMSA (Fig. 3B and C).

To verify the specificity of the DNase-protected sequence in the R region, a 25-bp double-stranded ODN (RF ODN) which contains the footprinted sequence was synthesized and used as a competitor for DNase footprinting and EMSA analysis. Figure 4B demonstrates specific competition of the footprint

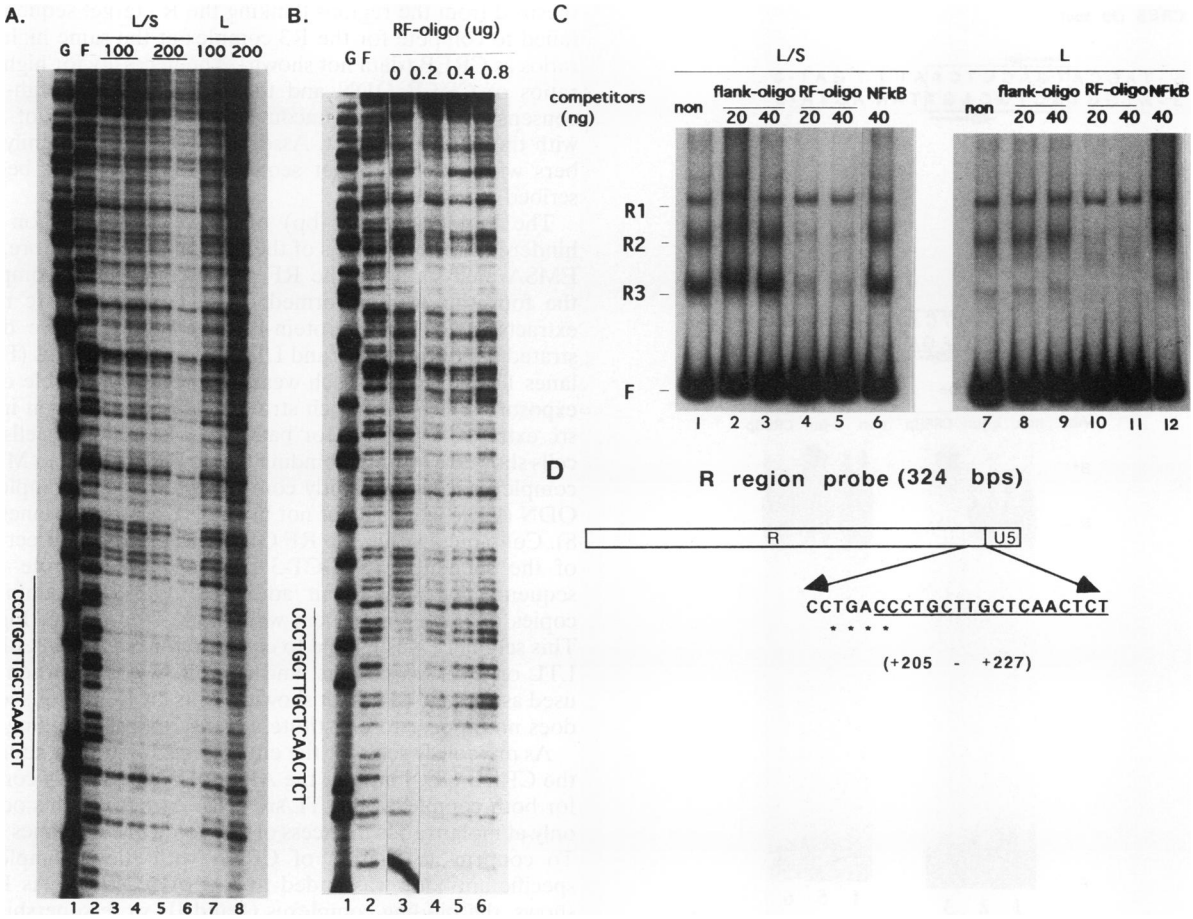

FIG. 4. Analysis of the R region suppressor site. (A) In vitro DNase I footprinting was performed on the end-labeled R region fragment. Lanes: 1, G ladder (Maxam-Gilbert reaction); 2, DNase I digestion of free probe; 3 to 6, 100 μg (lanes 3 and 4) and 200 μg (lanes 5 and 6) of LTL/src (L/S) nuclear extracts; 7 and 8, 100 and 200 μg of LTL (L) nuclear extract. The sequence of the protected region is indicated. (B) Specific competition of the footprint with increasing amounts of a double-stranded ODN which encompasses the protected sequence, 5′-CTGACCCT GCTTGCTCAACTCTGCG-3′ (footprinted sequence is underlined): 0 μg (lane 3), 200 μg (lane 4), 400 μg, (lane 5), and 800 μg (lane 6). (C) EMSA using the specific competitor as a probe. Lanes 1 to 6, LTL/src nuclear extract; lanes 7 to 12, LTL nuclear extract. The RF ODN (lanes 4 and 5) shows complete competition of the R3 complex, while a size-matched flanking region ODN, 5′-CTACCTAGACTCAGCCG GCTCTCCA-3′ (lanes 2 and 3), does not. NF-κB ODN (lane 6) and no competitor (lane 1) served as controls. The molar excesses of competitors are 50- and 100-fold (20 and 40 ng), respectively. The protein-DNA complexes are indicated as R1 to R3. (D) Sequence origin of the R region probe.

with increasing amount of this ODN. Similarly, the R3 complex in both LTL/src and LTL nuclear extracts was efficiently competed for by this ODN at 50- and 100-fold excess molar ratios (Fig. 4C). This finding suggests that the extracts contain a quantitative difference in the amount of the same suppressor factors. In contrast, the unrelated NF-κB ODN (Fig. 4C, lanes 6 and 12) as well as an upstream ODN which flanks the R region binding sequence cannot compete even at high molar ratios (Fig. 4C, lanes 2, 3, 8, and 9). The sequence and location of this protected region are shown in Fig. 4D. Interestingly, a CREB motif half-site (5′-TGAC-3′, indicated by asterisks) was found just adjacent to the footprinted region (underlined).

CREB binds to the R region suppressor target. The DNAse I-protected R region does not contain an obvious high-affinity CREB consensus sequence (Fig. 4D). Nevertheless, the results of okadaic acid, forskolin, H8, and Src studies (see above) strongly implicate a PKA-responsive transcription factor in suppression. This could occur as a direct or indirect effect of PKA. Since CREB-related family members are the best-characterized targets of PKA, we undertook studies to assess the involvement of CREB in the R region suppressor complex, R3. A high-affinity CREB ODN was synthesized as a probe (Fig. 5A). As a control, a closely related AP-1 ODN was also synthesized. The binding site of this ODN differed from that of CREB by only a single central nucleotide (Fig. 5A). Nevertheless, supershift analysis (Fig. 5B) showed binding of factors to these ODNs to be extremely specific, with c-Jun present only on the AP-1 ODN and CREB present only on the CREB ODN (compare lanes 2 and 3 and lanes 5 and 6).

When these two ODNs were used as competitors in EMSA analyses of the R region, CREB had a much greater effect than the AP-1 oligonucleotide in both LTL and LTL/src cells (Fig. 5C, lanes 4 versus 7 and 11 versus 13). In contrast, a control NF-κB ODN failed to compete at equivalent high molar ratios (Fig. 5C, lanes 8 and 14). Though competition was specific, it occurred only at very high molar ratios (up to 1,000-fold molar excess). Because of this, we performed control comparisons with an additional four size-matched ODN competitors syn-

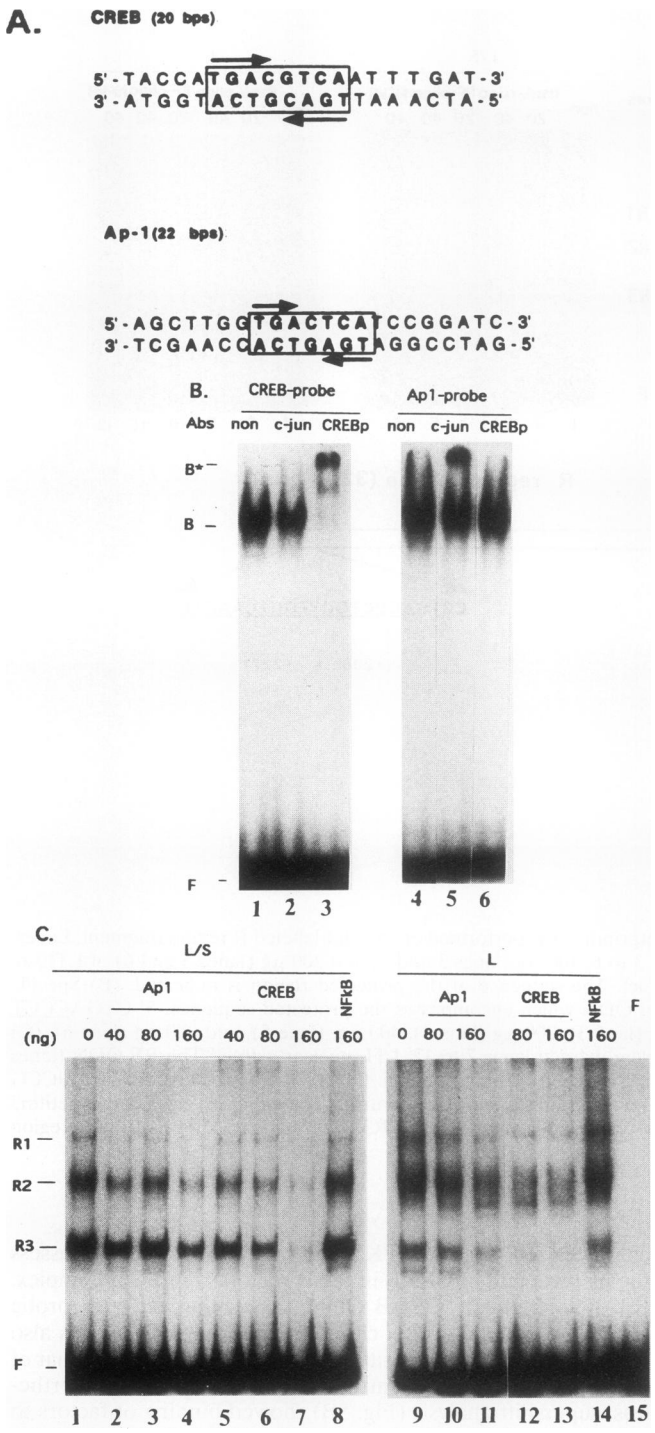

FIG. 5. Specific competition of R region binding by CREB ODN. (A) Schematic of high-affinity CREB and AP-1 double-stranded oligonucleotides. The binding motifs are boxed, and the arrows indicate symmetric palindromic sequences. (B) Specificity of CREB and AP-1 targets for binding factors demonstrated by EMSA supershift. Lanes: 1 to 3, CREB probe; 4 to 6, AP-1 probe. Two micrograms of specific antibodies (Abs) and 8 μg of LTL/src nuclear extracts were used for identification of bound proteins. c-Jun antibody (lanes 2 and 5) and CREB antibody (lanes 3 and 6) cause supershift only of the correct targets. B, high-affinity DNA-protein complex; B*, supershifted complex. No antibody controls are shown in lanes 1 and 4. (C) EMSA competition using the entire R region as a probe. Lanes: 1 to 8, LTL/src nuclear extracts; 9 to 14, LTL nuclear extracts; 15, free probe.

thesized from the regions flanking the R3 target sequence. All failed to compete for the R3 complex at the same high molar ratios as CREB (data not shown). The necessity for high molar ratios of CREB ODN and the lack of a clear high-affinity consensus suggests an unconventional interaction of CREB with the R region target. Associations of CREB family members with unusual target sequences have recently been described (53, 62).

The large size (324 bp) of the entire R region probe hindered further analysis of the R3 complex. Therefore, direct EMSA analysis using the RF probe (Fig. 4D) encompassing the footprint was performed on LTL and LTL/src nuclear extracts. Two major protein-DNA complexes were demonstrated in both the LTL and LTL/src nuclear extracts (Fig. 6A, lanes 1 and 5), with much weaker lower bands visible on long exposure. However, much stronger binding was seen in LTL/src extracts, especially for band II. Like LTL/src cells, MT4 cells showed a stronger binding to this RF probe than MT2. All complexes were efficiently competed for by the complete RF ODN (lanes 2 and 6) but not by the NF-κB ODN (lanes 4 and 8). Contained within the RF ODN was a twofold direct repeat of the sequence 5′-TGCT-3′. To address the role of this sequence in binding, an additional ODN containing four copies of this short repeat was synthesized (RF-c; Fig. 6A). This sequence was unable to compete for binding in either the LTL or LTL/src extracts, and no shift was seen when it was used as a probe (data not shown). Thus, by itself, this sequence does not appear to constitute a transcriptional binding motif.

As previously seen for the entire R region probe, addition of the CREB ODN but not the AP-1 ODN specifically competed for both complexes in LTL/src cells. As before, this occurred only at molar ratios in excess of 500-fold (Fig. 6B, lanes 2 to 5). To confirm association of CREB with these complexes, a specific antibody was added to EMSA reactions. As Fig. 6C shows, the binding complexes (I and II) were supershifted by CREB antibody (I* and II*) but not the control antibodies, anti-c-Jun and anti-NF-κB (Santa Cruz Biotechnology), demonstrating CREB involvement in the RF complex. Interestingly, there is also partial dissociation of binding by this antibody. Another CREB antibody (obtained from M. Montminy) led to complete dissociation of CREB from the RF complexes, forming a new low-molecular-weight complex (data not shown). As neither of these antibodies disturbs conventional CREB DNA binding or leucine zipper interactions, these data suggest that domains of CREB other than bZIP may be involved in the suppressor complex formation.

To test the relationship between the PKA pathway and the R region element in cells not transformed by *src*, we treated BALB/c 3T3 and LTL cells with a cAMP analog, dBcAMP. As shown in Fig. 6D, baseline BALB/c 3T3 and LTL nuclear extracts revealed no and weak binding activities, respectively (lanes 1 and 5). Specific binding was dramatically increased within 1 h of treatment with dBcAMP in both cell lines (lane 2 and 6). However, the augmented binding activity appeared to be transient, with a gradual decrease after 16 h of treatment. This is consistent with known kinetics of PKA activation (25). Activated BALB/c 3T3 nuclear extract showed an additional EMSA band after 1 h of treatment with dBcAMP (Fig. 6D,

The competition assays were performed by adding AP-1 oligonucleotide (lanes 2, 3, 4, 10, and 11), CREB ODN (lanes 5, 6, 7, 12, and 13), and NF-κB ODN (lanes 8 and 14). ODNs were added at 200-, 400-, and 800-fold molar excesses. Lanes 1 and 9 are controls in which no competitor oligonucleotide was added.

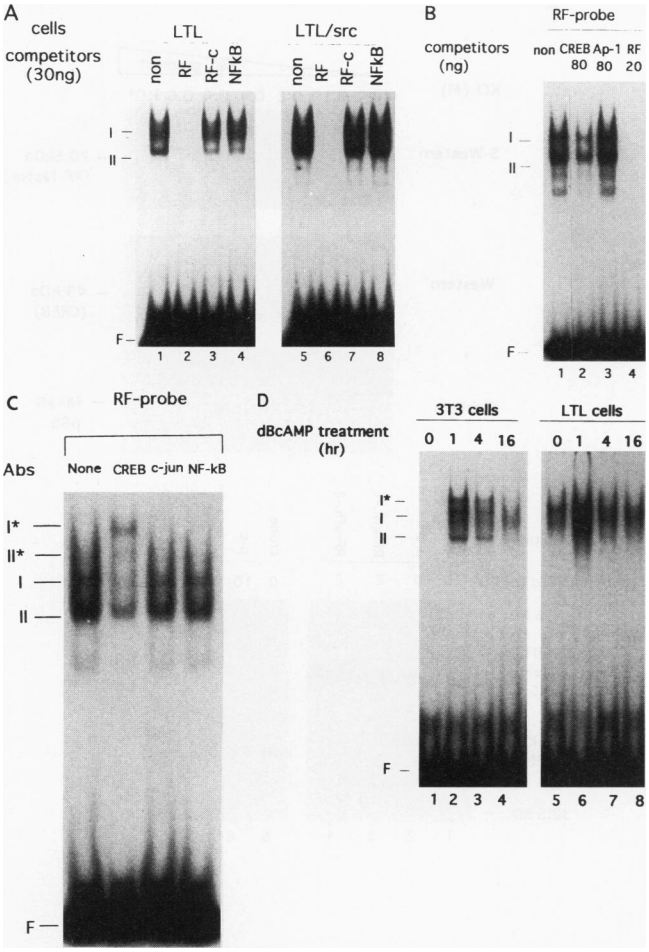

FIG. 6. EMSA analysis using the R region suppressor target (RF) as a probe. (A) Comparative EMSA of LTL (lane 1 to 4) and LTL/src (lane 5 to 8) extracts reveals increased binding in the *src*-transformed cells as previously shown for the whole R region probe. Unlabeled ODN competitors used are itself (lanes 2 and 6), a multimer of the direct repeat TGCT in the core (TGCTTGCTTGCTTGCT, RF-c; lanes 3 and 7), or NF-κB ODN (lanes 4 and 8). Competitors were added at the same time as the labeled probe. F, free probe. (B) The complexes can be competed for by CREB ODN (lane 2) but not by AP-1 ODN (lane 3). (C) Supershift assays using the RF probe. Specific antibodies (Abs) to CREB (lane 2), c-Jun (lane 3), and NF-κB (lane 4) were added. Lane 1, no-antibody control. Two more slowly migrating complexes are indicated as I* and II* with CREB antibody (lane 2). (D) EMSA with BALB/c 3T3 and LTL nuclear extracts after dBcAMP treatment (1 mM). Increased binding activity to the RF element and time course of treatment are indicated. A new binding band in dBcAMP-treated BALB/c 3T3 cells is indicated as I*.

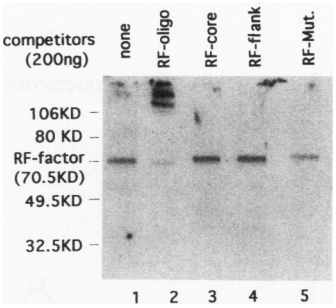

FIG. 7. Southwestern blot analysis with RF probe and competitor. Twenty micrograms of LTL/src crude nuclear extract was used per lane. The blotted membrane was cut into five strips and incubated with radiolabeled probe plus different competitors at a concentration of 100 ng/ml (100-fold molar excess). Lanes: 1, no competitor; 2, wild-type RF ODN; 3, RF core ODN (see Fig. 6); 4, RF flanking ODN (see Fig. 4); 5, RF mutant ODN (5′-CTGACCCTGCTTGCTCAAΔTCTGCG-3′; the replaced base [from C to A] is underlined).

lane 2), indicating interaction with additional transcription factors in this cell line (possibly other CREB family members, [see, for example, reference 33]).

A 70.5-kDa nuclear protein binds directly to the suppressor target, and CREB binds to it. A 70.5-kDa nuclear protein in LTL/src cell nuclear extracts was detected by Southwestern blot analysis using the short ^{32}P-labeled RF ODN as a probe (Fig. 7). No direct binding to CREB was seen. The specificity of p70 binding was confirmed by competition. As shown in Fig. 7, wild-type RF ODN specifically competed for binding, whereas the RF core and RF flanking region probes did not. An RF mutant ODN with one base substitution (Fig. 7) showed less effective competition than wild-type RF ODN. EMSA also confirmed at least 10-fold-decreased binding affinity to the mutant RF element (data not shown).

To better characterize the p70 DNA-binding protein in LTL/src cells, partial purification was performed. The crude nuclear extract was subjected first to phosphocellulose adsorption chromatography and then to high-stringency affinity purification over an RF ODN-containing column. Proteins were eluted from the RF affinity column by a 100 mM to 1 M KCl gradient (Fig. 8A). EMSA results suggested that the peak of the RF binding complex was eluted at 400 mM KCl (Fig. 8B), and the two fractions containing the binding activities were pooled. Quantitative measurement of their binding activities by EMSA revealed a purification of approximately 10-fold over that of phosphocellulose and about 100-fold over that of crude nuclear extracts. Results from Southwestern analysis also showed peak elution of the 70.5-kDa protein in the 400 mM KCl fraction. Thus, p70 protein concentration correlated well with total EMSA binding activity.

Interestingly, a 49-kDa CREB factor was coeluted with the 70.5-kDa protein only in the two 400 mM KCl fractions (Fig. 8C, middle panel). Subsequent Western blot analysis with monoclonal antibodies which distinguish CREB from CREM (provided by J. Hoeffler) showed that the copurified protein reacts like conventional CREB and not CREM. However, none of these antibodies react with p70. Thus, CREB appears unable to bind to the suppressor target by itself on Southwestern analysis (Fig. 8D, lanes 1 to 4).

To demonstrate specificity of the p70-CREB association, we analyzed the elution characteristics of an unrelated DNA-binding transcription factor, NF-κB p65 (to which we have obtained excellent antibodies from I. Verma). This protein was highly expressed in the nuclei of our cells (Fig. 8C, bottom panel) and, like CREB, coeluted from phosphocellulose at 400 mM. Neither CREB nor p65 was strongly enriched in the 400 mM phosphocellulose fraction in which p70 eluted, despite about 10-fold enrichment of p70 (Fig. 8D). Thus, the optimal phosphocellulose fractionation conditions for p70 capture only a subset of CREB and p65. However, in subsequent high-stringency affinity chromatography, both CREB and p70 showed approximately 10-fold stoichiometric enrichment (Fig. 8C and D; note that fivefold less total protein was loaded in last two lanes). In contrast to the CREB-p70 complex, p65 was completely lost. In additional experiments, coassociation oc-

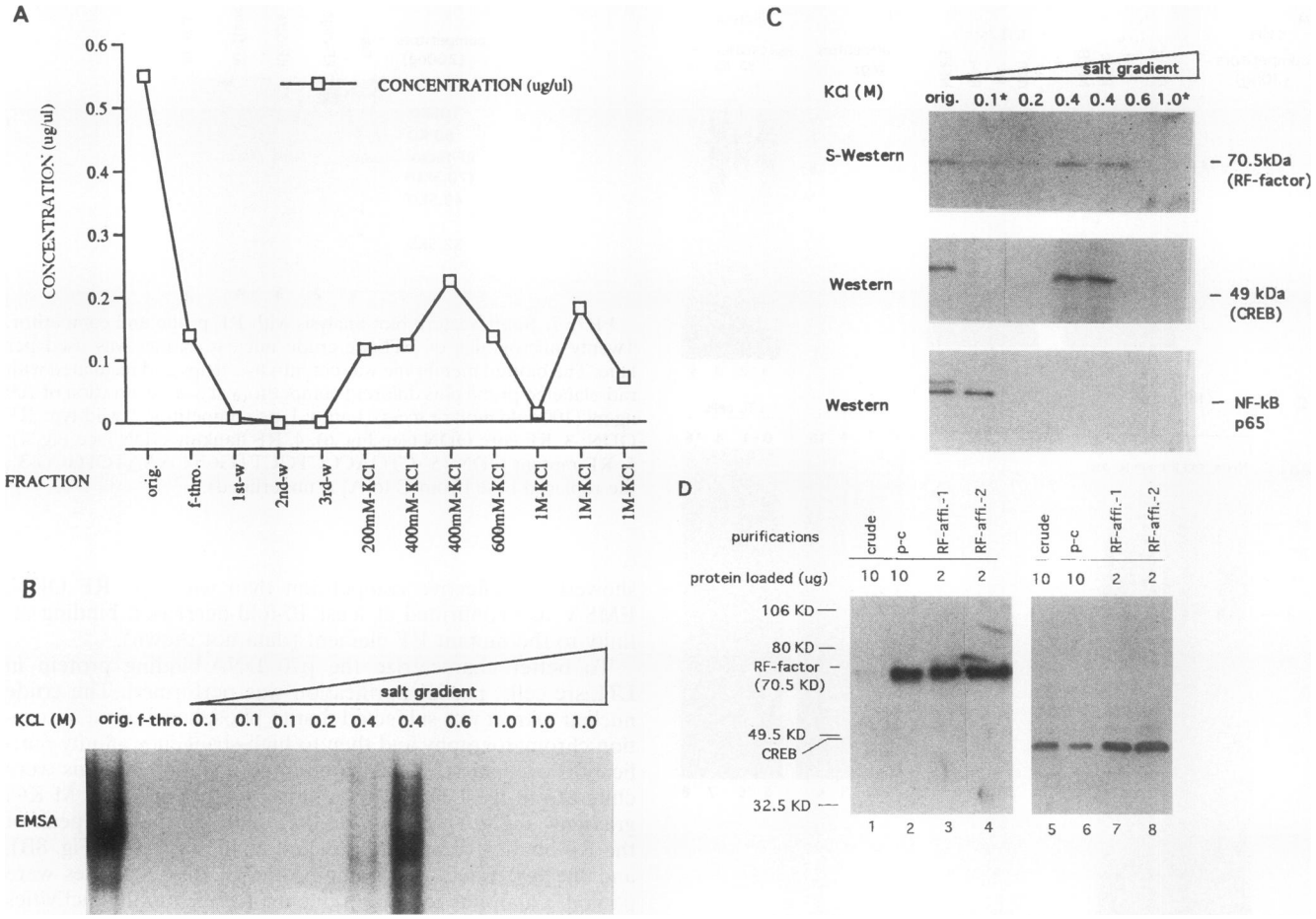

FIG. 8. RF affinity chromatography. Crude LTL/src nuclear extract was subjected first to phosphocellulose column fractionation and then to two cycles of RF affinity purification (see Materials and Methods). Results for the first cycle of purification are shown. (A) Protein concentrations of KCl gradient elutates measured by the Bradford protein assay (see Materials and Methods). Fraction are phosphocellulose-purified material (orig.), affinity column flowthrough (f-thro.), the first to third 100 mM KCl washes (1st-w to 3rd-w), and stepwise gradient elutions from 200 mM to 1 M KCl. (B) The binding activities of each fraction (as labeled) were screened by EMSA using the wild-type RF probe. (C) Parallel Southwestern blot analysis using the RF probe (top) and Western blot analysis with specific CREB and NF-κB p65 antibodies (middle and bottom) were performed to identify the contents of the factors binding to the RF ODN. The flowthrough and three 100 mM wash fractions were pooled (0.1*), as were the three 1 M KCl fractions (1.0*). p70 (RF factor), CREB protein, and NF-κB p65 are indicated. (D) Complex composition throughout purification, beginning with crude nuclear extract and ending with the second affinity purification. Blots of Southwestern analysis using the RF probe (lanes 1 to 4) and Western analysis using the CREB antibody (lanes 5 to 8) are shown. The amount of protein loaded from each purification step is indicated above the lanes: 10 μg of crude LTL/src nuclear extract (crude; lanes 1 and 5), 10 μg of phosphocellulose-purified LTL/src nuclear extract (p-c; lanes 2 and 6), and 2 μg of the first RF-affi.-1; lanes 3 and 7) and the 2 μg of the second (RF-affi.-2; lanes 4 and 8) RF affinity column-purified products. The 70.5-kDa protein (RF factor; lanes 1 to 4) and the 49-kDa CREB proteins (lanes 5 to 8) are indicated.

curred even when the extracts were exposed to 1 M KCl prior to the second round of affinity chromatography. Thus, like the supershift analysis, coelution through two cycles of affinity chromatography suggests tight association of p70 with CREB.

DISCUSSION

These data demonstrate the involvement of a CREB-like factor in the R region suppression complex and suggest direct interaction of this DNA-binding protein with an as yet unidentified 70.5-kDa R region suppressor. The CREB family of transcription factors is a highly diverse and degenerate family composed of multiple individual genes and splicing variants (23; reviewed in reference 33). These family members are capable of binding to conventional symmetric CRE target sites as well as highly variant sites (53, 62) in a variety of heterodimeric or homodimeric forms. Though the identity of the 70.5-kDa protein remains to be determined, we believe the 49.5-kDa protein to be CREB, based on the profile of antisera reactivity and comigration with conventional CREB from other cell lines. Further precise characterization will require direct sequencing. Analysis of the R region sequence failed to reveal a conventional high-affinity CREB binding site of the 5′-TGACGTCA-3′ type. Instead, a single 5′-TGAC-3′ half-site was found immediately upstream of the region footprinted in the LTL/src cells (Fig. 4D). The fact that the first three bases of this sequence, TGA, were not footprinted suggests at best a weak interaction through the DNA-binding domain of CREB at this site. Preliminary methylation interference data also suggest that the putative CREB half-site does not form an important DNA contact site (data not shown). In addition, extremely high concentrations of high-affinity CREB target

ODN are needed to disrupt the suppressor complex. This also suggests that the form of CREB involved in the complex has low affinity for a conventional CREB target. This would be very atypical for CREB homodimers (or heterodimers with related family members). Western blot analyses demonstrate no increase in the total or nuclear concentrations of CREB in the LTL/src cells (unpublished data). However, supershift analyses suggest that more CREB is present on the suppressor target in the LTL/src cells than the LTL cells. The ability of the high-affinity CREB competitor to decrease the quantity but not mobility of the suppressor complex suggests there may be a relatively tight interaction of CREB with the rest of the R region complex. Coelution studies also suggest this. In contrast, the mobility of the complex is readily affected by antibodies to CREB. Antibody apparently supershifted the R region complex; furthermore, a CREB protein was copurified with RF factor through the RF affinity chromatography. These data strongly suggest the involvement of CREB protein in forming the complex which subsequently suppresses the HTLV-I LTR promoter.

However, results from Southwestern blot analysis performed under reducing conditions demonstrated that the 70.5-kDa DNA-binding protein can efficiently bind to the RF element by itself, whereas no direct binding to CREB was seen. This suggests that CREB may not necessarily contribute to the basic affinity of the underlying complex for DNA. However, the exact mechanisms by which CREB functionally or physically interacts with the 70.5-kDa protein will have to await in vitro reconstitution with the cloned factors.

Unchanged protein-DNA complexes in U3 despite profound changes in the R region suggest that CREB-associated suppression is R region specific. An 18-bp element between +209 and +226 is specifically footprinted during suppression. In other studies which linked the R region to a heterologous simian virus 40 promoter, augmented expression was seen. The region conferring up-modulation was narrowed down to nucleotide positions +205 to +240 by deletion assay (39). The ability of this sequence to serve as a repressor or activator is likely determined by other neighborhood proteins. Alternatively, the spacing between the R region and the promoter may be crucial. CREB-associated upstream suppression has precedent. For example, the transcriptional inhibition of the glycoprotein hormone α-subunit gene by the glucocorticoid receptor is effective only when the glucocorticoid receptor directly or indirectly interacts with CREB (58).

Transcriptional suppression by protein interaction with sequences downstream of the RNA initiation site has also been demonstrated in other virus and cellular genes (4, 10, 15, 28, 50). For example, the suppression of herpes simplex virus latency-associated transcripts is conferred by a 55-bp region downstream of the TATA box (10). In the adenovirus type 5 E1A promoter, down-regulation was observed in response to a single-base deletion downstream of the transcription start site (28).

The choice between productive and latent infection of HTLV-I may be determined by a balance between positively acting viral and host factors with negatively acting host suppressors. The LTR promoter was latent in transgenic mouse thymocytes and splenocytes but could readily be activated either through constitutive *tax* expression via introduction of the Thy-*tax* transgene (43) or by activating the cellular PKC pathway with phorbol myristate acetate plus inomycin (6). These results suggest that breakage of transcriptional latency may occur through direct activation of the LTR promoter by *tax* or by transacting PKC-responsive cellular transcriptional factors such as AP-1, Sp-1, or Ets (21). Transformation of fibroblasts by *tax* induces suppression of the β-Gal transgene even in the presence of Tax protein, and both transgenes (*tax* and β-Gal) may be suppressed by *src*. Thus, regulation of HTLV-I latency involves both positive regulation and active suppression of the LTR through different pathways. This may confer selective advantage for the virus. Up-modulation through U3 targets may ensure rapid and efficient transmission to a new host. Subsequent suppression through the R region may then prevent elimination of the virus by the immune system and may explain why HTLV-I expression after infection is so rarely seen. The rare cases in which leukemia or tropical spastic paraparesis/HTLV-I-associated myelopathy develops likely represent aberrancies in this tight system of regulation.

ACKNOWLEDGMENTS

We thank M. Montminy, I. Verma, S. Oroszlan, L. Bibbs, C. Lai, and J. Hoeffler for supplying reagents, L. Whitton and M. Wilson for advice, and M. Duncan for assistance with manuscript preparation.

This work was supported by grants CA50234, MH47680, and NS01330 to M.I.N. D.A.B. was supported by the California Universitywide AIDS Research Program.

REFERENCES

1. **Akerblom, I. E., E. P. Slater, M. Beato, J. D. Baxter, and P. L. Mellon.** 1988. Negative regulation by gucocorticoids through interference with a cAMP responsive enhancer. Science. **241**:350–353.
2. **Ausubel, F. M., R. Brent, R. E. Kingston, D. D. Moore, J. G. Seidman, J. A. Smith, and K. Struhl (ed.).** 1992. Current protocols in molecular biology, p. 12.4. Greene Publishing Associates and Wiley-Interscience, New York.
3. **Ardrisani, D., and J. E. Dixon.** 1990. Identification and purification of a novel 120-kDa protein that recognizes the cAMP-responsive element. J. Biol. Chem. **265**:3212–3218.
4. **Arya, S. K.** 1991. Human immunodeficiency type 2 (HIV-2) gene expression: downmodulation by sequence elements downstream of the transcriptional initiation site. AIDS Res. Hum. Retroviruses **12**:1007–1014.
5. **Brown, D.** Unpublished data.
6. **Brown, D. A., X. Xu, I. Kitajima, T. Shinohara, J. Bilakovics, T. Shiner, and M. I. Nerenberg.** Genomic footprinting of the HTLV-I LTR in a transgenic mouse tymorigenesis model. Transgene, in press.
7. **Brown, D., et al.** Unpublished data.
8. **Brown, D. A., K. L. Kondo, S. W. Wong, and D. J. Diamond.** 1992. Characterization of nuclear protein binding to the interferon-γ promoter in quiescent and activated human T cells. Eur. J. Immunol. **22**:2419–2428.
9. **Badley, J. E., G. A. Bishop, T. St. John, and J. A. Frelinger.** 1988. A simple, rapid method for the purification of poly A^+ RNA. BioTechniques **6**:114–116.
10. **Bathchelor, A. H., and P. O'Hare.** 1990. Regulation and cell-type-specific activity of a promoter located upstream of the latency-associated transcript of herpes simplex virus type 1. J. Virol. **64**:3264–3279.
11. **Bosselut, R., J. F. Duvall, A. Gegonne, M. Baily, A. Hemar, J. Brady, and J. Ghysdael.** 1990. The product of the c-ets-1 proto-oncogene and the related Ets2 protein act as transcriptional activators of the long terminal repeat of human T-cell leukemia virus HTLV-1. EMBO J. **9**:3137–3144.
12. **Brott, B. K., S. Decker, M. C. O'Brien, and R. Jove.** 1991. Molecular features of the viral and cellular src kinase involved in interactions with the GTPase-activating protein. Mol. Cell. Biol. **11**:5059–5067.
13. **Bushman, W. A., L. K. Wilson, D. K. Luttrell, J. S. Moyers, and S. J. Parsons.** 1990. Overexpression of c-src enhances β-adrenergic-induced cAMP accumulation. Proc. Natl. Acad. Sci. USA **87**:7462–7466.
14. **Copeland, N. G., A. D. Zelenetz, and G. M. Cooper.** 1980. Transformation by subgenomic fragments of P Rous sarcoma virus DNA. Cell **19**:863–870.

15. **Farabaugh, P. J., A. Vimaladithan, S. Türkel, R. Johnson, and H. Zhao.** 1993. Three downstream sites repress transcription of a Ty2 retrotransposon in *Saccharomyces cerevisiae*. Mol. Cell. Biol. **13:** 2081–2090.
16. **Franchini, G., F. Wong-Staal, and R. C. Gallo.** 1984. Human T-cell leukemia virus (HTLV-I) transcripts in fresh and cultured cells of patients with adult T-cell leukemia. Proc. Natl. Acad. Sci. USA **81:**6207–6211.
17. **Franklin, A. A., M. F. Kubik, M. N. Uittenbogaard, A. Brauweiler, P. Utaisincharoen, M. A. Matthews, W. S. Dynan, J. P. Hoeffler, and J. K. Nyborg.** 1993. Transcription by human T-cell leukemia virus TAX protein is mediated through enhanced binding of activating transcription factor-2 (ATF-2) ATF-2 response and cAMP element-binding protein (CREB). J. Biol. Chem. **268:** 21225–21231.
18. **Fujisawa, J. I., M. Toita, and M. Yoshida.** 1989. A unique enhancer element for the *trans* activator ($p40^{tax}$) of human T-cell leukemia virus type I that is distinct from cyclic AMP- and 12-*O*-tetradenoylphorbol-13-acetate-responsive elements. J. Virol. **63:**3234–3239.
19. **Garica, R., N. U. Parikh, H. Saya, and G. E. Gallick.** 1991. Effect of herbimycin A on growth and $pp60^{c\text{-}src}$ activity in human colon tumor cell lines. Oncogene **6:**1983–1989.
20. **Gartenhaus, R. B., F. Wong-Staal, and M. E. Klotman.** 1991. The promoter of human T-cell leukemia virus type-I is repressed by the immediate-early gene region of human cytomegalovirus in primary blood. Blood **78:**2956–2961.
21. **Gegonne, A., R. Bosselut, R. A. Bailly, and J. Ghysdaal.** 1993. Synergistic activation of the HTLV1 LTR ets-responsive region by transcription factors ets1 and Sp1. EMBO J. **2:**1169–1178.
22. **Gitlin, S. D., J. Dittmer, R. L. Reid, and J. N. Brady.** 1993. The molecular biology of human T-cell leukemia viruses, p. 159–192. *In* B. Cullen (ed.), Frontier in molecular biology. Oxford University Press, Oxford.
23. **Habener, J. F.** 1990. Cyclic AMP response element binding protein: a cornucopia of transcription factors. Mol. Endocrinol. **4:**1087–1094.
24. **Hansen, M. B., S. E. Nielsen, and K. Berg.** 1989. Re-examination and further development of a precise and rapid dye method for measuring cell growth/cell kill. J. Immunol. Methods **119:**203–210.
25. **Hemmings, B. A.** 1986. cAMP mediated proteolysis of the catalytic subunit of cAMP-dependent protein kinase. FEBS Lett. **196:**126–130.
26. **Hidaka, H., M. Inagaki, S. Kawamoto, and Y. Sasaki.** 1984. Isoquinolinesulfonamides, novel and potent inhibitors of cyclic nucleotide dependent protein kinase and protein kinase C. Biochemistry **23:**5036–5041.
27. **Hinrich, S. H., M. I. Nerenberg, R. K. Reynolds, G. Khoury, and G. Jay.** 1987. A transgenic mouse model for human neurofibromatosis. Science **237:**1340–1343.
28. **Ho, D. Y.** 1992. Herpes simplex virus latency: molecular aspects. Prog. Med. Virol. **39:**76–115.
29. **Kadonaga, J. T., and R. Tijian.** 1986. Affinity purification of sequence specific DNA binding proteins. Proc. Natl. Acad. Sci. USA **83:**5889–5893.
30. **Kashanchi, F., J. F. Duvall, P. F. Lindholm, M. F. Radonovich, and J. N. Brady.** 1993. Sequences downstream of the RNA initiation site regulate human T-cell lymphotropic virus type I basal gene expression. J. Virol. **67:**2894–2902.
31. **Kitajima, I., T. Shinohara, J. Bilokovics, D. A. Brown, X. Xu, and M. I. Nerenberg.** 1992. Ablation of transplated HTLV-I tax-transformed tumors in mice by antisense inhibition of NF-κB. Science **258:**1792–1795.
32. **Kitajima, I., T. Shinohara, T. Minor, L. Bibbs, J. Bilakovics, and M. I. Nerenberg.** 1992. Human T-cell leukemia virus type I tax transformation is associated with increased uptake of oligodeoxynucleotides in vitro and in vivo. J. Biol. Chem. **267:**25881–25888.
33. **Kwast-Welfeld, J., I. de Bell, P. R. Walker, J. F. Whitfield, and M. Sikorska.** 1993. Identification of a new cAMP response element-binding factor by Southwestern blotting. J. Biol. Chem. **268:**19581–19585.
34. **Levinger, L., and J. A. Lautenberger.** 1987. Human protein binding to DNA sequences surrounding the human T-cell lymphotropic virus type I long terminal repeat polyadenylation site. Eur. J. Biochem. **166:**519–526.
35. **MacGregor, G. R., G. P. Nolan, S. Fiering, M. Roederer, and L. A. Herzenberg.** 1989. Use of E. Coli lac Z (β-galactosidase) as a reporter gene. Methods Mol. Biol. **7:**217–235.
36. **Miyoshi, I., I. Kubonishi, S. Yoshimoto, T. Akagi, Y. Ohtsuki, Y. Shiraishi, K. Nagata, and Y. Hinuma.** 1981. Type C virus particles in a cord-cell line derived by co-cultivating normal human cord leukocytes and human leukaemic T cells. Nature (London) **294:** 770–771.
37. **Moyers, J., A. H. Bouton, and S. J. Parsons.** 1993. The sites of phosphorylation by protein kinase C and an intact SH2 domain are required for the enhanced response to β-adrenergic agonists in cells overexpressing c-*src*. Mol. Cell. Biol. **13:**2391–2400.
38. **Muchardt, C., J. S. Seeler, A. Nirula, S. Gong, and R. Gaynor.** 1992. Transcription factor AP-2 activates gene expression of HTLV-I. EMBO J. **12:**2573–2581.
39. **Nakamura, M., K. Ohtani, Y. Hinuma, and K. Sugamula.** 1988. Functional mapping of the activity of the R region in the human T-cell leukemia virus type I long terminal repeat to increase gene expression. Virus Genes **2:**147–155.
40. **Nerenberg, M. I.** 1992. Biological and molecular aspects of HTLV-I-associated diseases, p. 225–247. *In* R. Roos (ed.), Molecular neurovirology. Humana Press Inc., Totowa, N.J.
41. **Nerenberg, M. I., H. Hinrichs, R. K. Reynolds, G. Khoury, and G. Jay.** 1987. The tat gene of human T-cell lymphotropic virus type-I induces mesenchymal tumors in transgenic mice. Science **237:** 1324–1329.
42. **Nerenberg, M., and G. Jay.** 1989. Expression of HTLV-I in transgenic mice, p. 170–176. *In* A. L. Notkins and M. B. A. Oldstone (ed.), Concepts in viral pathogenesis, vol. III. Springer-Verlag, New York.
43. **Nerenberg, M. I., T. Minor, J. Price, D. N. Ernst, T. Shinohara, and H. Schwarz.** 1991. Transgenic thymocytes are refractory to transformation by the human T-cell leukemia virus type I *tax* gene. J. Virol. **65:**3349–3353.
44. **Nerenberg, M. I., and C. A. Wiley.** 1989. Degeneration of oxidative muscle fibers in HTLV-1 transgenic mice. Am. J. Pathol. **135:** 1025–1033.
45. **Nichols, M., F. Weih, W. Schmid, C. deVack, E. Kowenz-Leutz, B. Luckow, M. Boshart, and G. Schutz.** 1992. Phosphorylation of CREB affects its binding to high and low affinity sites: implications for cAMP induced gene transcription. EMBO J. **11:**3337–3346.
46. **Niki, M., K. Ohtani, M. Nakamura, and K. Sugamura.** 1992. Multistep regulation of enhancer activity of the 21-base-pair element of human T-cell leukemia virus type I. J. Virol. **66:**4348–4357.
47. **Nyborg, J. K., M. A. Matthews, J. Yucel, W. T. Golde, W. S. Dynan, and W. Wachsman.** 1990. Interaction of host cell proteins with the human T-cell leukemia virus type I transcriptional control region. J. Biol. Chem. **265:**8237–8242.
48. **Olashaw, N. E., and W. J. Pledger.** 1988. Cellular mechanisms regulating proliferation. Adv. Second Messenger Phosphoprotein Res. **12:**139–155.
49. **Paskalis, H., B. K. Felber, and G. N. Pavlakis.** 1986. Cis-acting sequences responsible for the transcriptional activation of human T-cell leukemia virus I constitute a conditional enhancer. Proc. Natl. Acad. Sci. USA **83:**6558–6562.
50. **Pierani, A. C. Pouponnot, and G. Calothy.** 1993. Transcriptional downregulation of the retina-specific QR1 gene by $pp60^{v\text{-}src}$ and identification of a novel v-*src*-responsive unit. Mol. Cell. Biol. **13:**3401–3414.
51. **Qureshi, S. A., C. K. Josegh, M. Rim, A. Maroney, and D. Foster.** 1991. v-Src activates both protein kinase C-dependent and independent signaling pathways in murine fibroblasts. Oncogene **6:**995–999.
52. **Risse, G., K. Jooss, M. Neuberg, H. J. Bruller, and R. Muller.** 1989. Asymmetrical recognition of the palindromic AP1 binding site (TRE) by Fos protein complexes. EMBO J. **8:**3825–3832.
53. **Rodland, K. D., D. Pribow, P. Lenormand, S. L. Chen, and B. E. Magun.** 1993. Characterization of a unique enhancer element responsive to cyclic AMP and elevated calcium. Mol. Endocrinol. **7:**787–796.

54. **Rosen, C., J. G. Sodroski, and W. A. Haseltine.** 1985. Location of cis-acting regulatory sequences in the human T-cell leukemia virus type I long terminal repeat. Proc. Natl. Acad. Sci. USA **82**:6502–6506.
55. **Saggioro, D., M. Panozzo, and L. Chieco-Bianchi.** 1990. Human T-lymphotropic virus type I transcriptional regulation by methylation. Cancer Res. **50**:4968–4973.
56. **Salahuddin, S. Z., P. D. Markham, F. Wong-Staal, G. Franchini, V. S. Kalyanaraman, and R. C. Gallo.** 1983. Restricted expression of human T-cell leukemia virus (HTLV) in transformed human umbilical cord blood lymphocytes. Virology **129**:51–64.
57. **Shalloway, D., A. D. Zelenetz, and G. M. Cooper.** 1981. Molecular cloning and characterization of the chicken gene homologous to the transforming gene of Rous sarcoma virus. Cell **24**:531–541.
58. **Stauber, C., J. Altschmied, I. E. Akerblom, J. L. Maron, and P. L. Mellon.** 1992. Mutual cross-interference between glucocorticoid receptor and CREB inhibits transactivation in placental cells. New Biol. **4**:527–540.
59. **Stagg, R. B., and W. H. Fletcher.** 1990. The hormone-induced regulation of contact-dependent cell-cell communication by phosphorylation. Endocrine Rev. **11**:302–325.
60. **Suzuki, T., J. Fujisawa, M. Toita, and M. Yoshida.** 1993. The trans-activator tax of human T-cell leukemia virus type I (HTLV-I) interacts with cAMP-responsive element (CRE) binding and CRE modulator proteins that bind to the 21-base-pair enhancer. Proc. Natl. Acad. Sci. USA **90**:610–614.
61. **Tachibana, K., P. J. Scheur, Y. Tsykiani, H. Kikuchi, D. Van Engen, J. Clardy, Y. Gopichand, and F. J. Schmitz.** 1981. Okadaic acid, a cytotoxic polyether from two marine sponges of the genus Halichondria. J. Am. Chem. Soc. **103**:2465–2471.
62. **Vallejo, M., L. Penchuk, and J. F. Habener.** 1992. Somatostatin gene upstream enhancer element activated by a protein complex consisting of CREB, Isl-1-like, and a-CBF-like transcription factors. J. Biol. Chem. **267**:12876–12884.
63. **Wagner, S., and M. R. Green.** 1993. HTLV-I Tax protein stimulation of DNA binding of bZIP proteins by enhancing dimerization. Science **262**:395–399.
64. **Yoshida, M., I. Miyoshi, and Y. Hinuma.** 1982. Isolation and characterization of retrovirus from cell lines of human adult T-cell leukemia and its implication in the disease. Proc. Natl. Acad. Sci. USA **79**:2031–2035.
65. **Yoshida, M., M. Osame, K. Usuku, M. Matsumoto, and A. Igata.** 1987. Viruses detected in HTLV-I associated myelopathy and adult T-cell leukemia are identical in DNA blotting. Lancet **1**:1085–1086.
66. **Yoshimura, T., J. Fujisawa, and M. Yoshida.** 1990. Multiple cDNA clones encoding nuclear proteins that bind to the tax-dependent enhancer of HTLV-I: all contain a leucine zipper structure and basic amino acid domain. EMBO J. **9**:2537–2542.